

(4)

AD-A203
933

Mutual Coherence of Two Coupled Multiline Continuous-Wave HF Lasers

J. M. BERNARD, R. A. CHODZKO, and H. MIRELS
Aerophysics Laboratory
Laboratory Operations
The Aerospace Corporation
El Segundo, CA 90245

7 December 1988

Prepared for
AIR FORCE WEAPONS LABORATORY
Kirtland Air Force Base, NM 87117

SPACE DIVISION
AIR FORCE SYSTEMS COMMAND
Los Angeles Air Force Base
P.O. Box 92960
Los Angeles, CA 90009-2960

DTIC
ELECTED
14 FEB 1989
S E D
 α_E

APPROVED FOR PUBLIC RELEASE.
DISTRIBUTION UNLIMITED

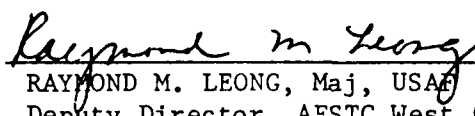
This report was submitted by The Aerospace Corporation, El Segundo, CA 90245, under Contract No. F04701-85-C-0086 with the Space Division, P.O. Box 92960, Los Angeles, CA 90009-2960. It was reviewed and approved for The Aerospace Corporation by W. P. Thompson, Jr., Director, Aerophysics Laboratory. Lt. Scott W. Levinson, SD/CNW, was the Air Force project officer.

This report has been reviewed by the Public Affairs Office (PAS) and is releasable to the National Technical Information Service (NTIS). At NTIS, it will be available to the general public, including foreign nationals.

This technical report has been reviewed and is approved for publication. Publication of this report does not constitute Air Force approval of the report's findings or conclusions. It is published only for the exchange and stimulation of ideas.



SCOTT W. LEVINSON, Lt, USAF
Project Officer
SD/CNW



RAYMOND M. LEONG, Maj, USAF
Deputy Director, AFSTC West Coast Office
AFSTC/WCO OL-AB

UNCLASSIFIED

SECURITY CLASSIFICATION OF THIS PAGE

REPORT DOCUMENTATION PAGE

1a. REPORT SECURITY CLASSIFICATION Unclassified		1b. RESTRICTIVE MARKINGS	
2a. SECURITY CLASSIFICATION AUTHORITY		3. DISTRIBUTION/AVAILABILITY OF REPORT Approved for public release; distribution unlimited.	
2b. DECLASSIFICATION / DOWNGRADING SCHEDULE			
4. PERFORMING ORGANIZATION REPORT NUMBER(S) TR-0086(6060)-5		5. MONITORING ORGANIZATION REPORT NUMBER(S) SD-TR-88-105	
6a. NAME OF PERFORMING ORGANIZATION The Aerospace Corporation Laboratory Operations	6b. OFFICE SYMBOL (If applicable)	7a. NAME OF MONITORING ORGANIZATION Space Division	
6c. ADDRESS (City, State, and ZIP Code) El Segundo, CA 90245		7b. ADDRESS (City, State, and ZIP Code) Los Angeles Air Force Base Los Angeles, CA 90009-2960	
8a. NAME OF FUNDING/SPONSORING ORGANIZATION Air Force Weapons Laboratory	8b. OFFICE SYMBOL (If applicable)	9. PROCUREMENT INSTRUMENT IDENTIFICATION NUMBER F04701-85-C-0086	
8c. ADDRESS (City, State, and ZIP Code) Kirtland Air Force Base, NM 87117		10. SOURCE OF FUNDING NUMBERS	
		PROGRAM ELEMENT NO.	PROJECT NO.
		TASK NO.	WORK UNIT ACCESSION NO.
11. TITLE (Include Security Classification) Mutual Coherence of Two Coupled Multiline Continuous-Wave HF Lasers			
12. PERSONAL AUTHOR(S) Bernard, Jay M.; Chodzko, Richard A.; and Mirels, Harold			
13a. TYPE OF REPORT	13b. TIME COVERED FROM _____ TO _____	14. DATE OF REPORT (Year, Month, Day) 1988 December 7	15. PAGE COUNT 12
16. SUPPLEMENTARY NOTATION			
17. COSATI CODES		18. SUBJECT TERMS (Continue on reverse if necessary and identify by block number) Lasers Resonators Phased array	
19. ABSTRACT (Continue on reverse if necessary and identify by block number) Two multiline cw HF lasers employing unstable resonators were coupled by injecting 20% of each laser output into the other laser. The mutual coherence of the two output beams was measured by recording the visibility V of the interference fringes generated when the beams are overlapped. Both single-line and multiline interference patterns were observed. The output from the two lasers in the present experiment (20% coupling) was completely coupled, indicating that the achievement of stable coupling is not dependent on careful adjustment of the length of each laser resonator.			
20. DISTRIBUTION/AVAILABILITY OF ABSTRACT <input type="checkbox"/> UNCLASSIFIED/UNLIMITED <input checked="" type="checkbox"/> SAME AS RPT <input type="checkbox"/> DTIC USERS		21. ABSTRACT SECURITY CLASSIFICATION Unclassified	
22a. NAME OF RESPONSIBLE INDIVIDUAL		22b. TELEPHONE (Include Area Code)	22c. OFFICE SYMBOL

FIGURES

1. Schematic diagram of coupled unstable resonators and near-field fringe diagnostics..... 4
2. Expanded thermal image of multiline near-field fringes..... 7
3. Oscilloscope traces of multiline near-field scans..... 7
4. Oscilloscope trace of P₂(6) single-line fringe pattern..... 8

Accession For	
NTIS GRA&I	
DTIC TAB	
Unannounced	
Justification	
By _____	
Distribution/	
Availability Codes	
Dist	Avail and/or Special
A-1	



We consider the coupling of two nominally identical lasers by partial injection of the output from each laser into the other. When steady-state coupling is achieved and the output beams are in phase, the beams can be used to form a phased array.¹ The stability of this system was investigated theoretically by Spencer and Lamb² for a single laser transition. It was found that steady-state coupled operation is achieved when the length of each laser resonator is adjusted so that the empty-cavity frequency is the same for each resonator. A perturbation of one resonator length resulted in reduced stability and ultimately uncoupled operation. Analytic expressions for allowable length perturbations (i.e., lock-in range) are presented by Chow.³

Spencer and Lamb's theory was experimentally confirmed by Palma and Fader¹ with a CO₂ laser. More recently, their theory was generalized to account for arbitrary-length separation between the two coupled lasers.⁴ The conclusion was that, in general, it is not possible to achieve steady-state operation on all potential laser transitions for multiline lasers. However, the effect of mode competition was not considered.

Here, we report initial results from an experimental study that addressed two major technical questions on the performance of two coupled multiline cw HF chemical lasers with unstable resonators: (1) Is it necessary that the two resonators have the same length (to within a fraction of a wavelength) to achieve steady-state coupling? and (2) Is the output coupled for some laser transitions and uncoupled for others?

The test apparatus is diagrammed schematically in Fig. 1. Mirrors M₁-M₂ and M₃-M₄ constitute two nominally identical confocal unstable resonators (length L = 1.5 m, mode diameter = 1 cm, magnification M = 1.4, and equivalent Fresnel number 4.1). They are assembled to enclose a supersonic-diffusion HF gain generator⁵ (maximum gain-length product g₀l = 1.8), so that the two 1-cm-diameter resonator modes are separated vertically by 0.5 cm in the gain region. Coupled or not, the major laser transitions and relative output powers are

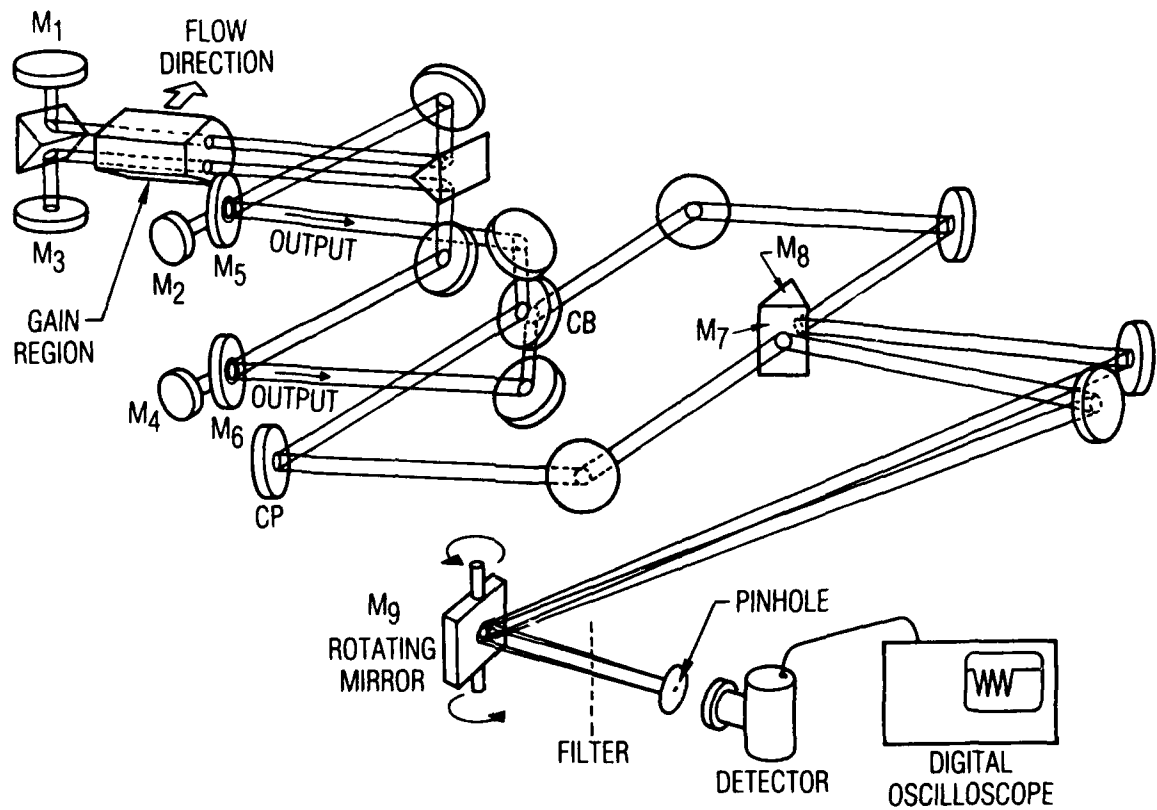


Fig. 1. Schematic diagram of coupled unstable resonators and near-field fringe diagnostics.

$P_1(5)$:	12%	$P_2(5)$:	14%
$P_1(7)$:	2%	$P_2(6)$:	36%
$P_1(9)$:	1%	$P_2(7)$:	29%
$P_2(3)$:	0.5%	$P_2(8)$:	3%
$P_2(4)$:	1.5%		

When coupled, each of the two laser outputs, from hole-scraper mirrors M_5 and M_6 , is directed into the other's resonator through the ZnSe-coupling beam splitter, CB (20% transmission, 80% reflection at one surface and an antireflection coating at the second surface).

The coupling path length between M_5 and M_6 also is approximately 1.5 m. The two laser outputs emerge as the reflection from the coupling beam splitter. A ZnSe-compensating plate, CP, is used in the path of the upper laser output because of the dispersion encountered by the lower laser output, which travels through the coupling beam splitter before being reflected. The laser outputs are directed to mirrors M_7 and M_8 , which become the synthetic aperture for the coupled laser system. These two outputs are made to overlap at an angle of 2 mrad in the near field to produce a pattern of linear interference fringes. Note that fringes appear only if the two outputs are phase related. The fringe pattern is observed on a thermal image screen. It is also translated past a pinhole-detector combination by rotating mirror M_9 and is recorded by an oscilloscope. The oscilloscope trace depicts intensity versus distance along a line perpendicular to the fringes. A filter is placed in front of the pinhole (Fig. 1) to obtain the fringe pattern corresponding to a single laser line.

Fringe visibility V can be deduced from the oscilloscope traces, namely,

$$V = \frac{(I_{\max} - I_{\min})}{(I_{\max} + I_{\min})}$$

where I_{\max} and I_{\min} are the maximum and minimum voltage levels, respectively, above the zero-intensity baseline on the oscilloscope trace. A fringe visibility of 1 corresponds to complete coupling and phase coherence of the two lasers, whereas $V = 0$ implies that the lasers are operating independently.

An enlarged thermal image of the multiline fringe pattern is shown in Fig. 2 for two values of the length of the lower resonator. The appearance of fringes at every cavity length that we tried demonstrates that at least a portion of the output of the two lasers can be coupled without precisely controlling cavity length. The uniformity of the fringes indicates perfect phase coherence of the coupled beams throughout the interaction region.

A typical oscilloscope trace of the upper and lower output beams, and of the multiline fringe pattern, is shown in Fig. 3. In this figure, $V = 0.6$, which implies either incomplete coupling or unequal optical paths for the two beams. To determine whether complete coupling is occurring (i.e., all output power is coupled), it is necessary to either equalize resonator and external optical path length or to measure, separately, the fringe visibility for each line of the multiline interference pattern.

Filters were available that enabled the interference patterns for $P_1(5)$ and $P_2(6)$ to be inspected. A typical fringe pattern for $P_2(6)$ is shown in Fig. 4. For several such traces, the measured visibility was $V = 0.90 \pm 0.02$. After correcting for the finite size of the pinhole relative to the fringe-separation distance, an experimental value of $V = 1.0$ was indicated. Hence, it may be concluded that the laser transition $P_2(6)$ is completely coupled. This result was obtained for both $P_1(5)$ and $P_2(6)$ from a number of tests, which included coarse (millimeter) perturbations of resonator length. Since these two lines may be considered to be typical lasing transitions, it is concluded that, for the 20% coupling, the entire output for both lasers is coupled and the achievement of stable coupling is insensitive to resonator-length equalization. Moreover, the value $V \neq 1$ deduced from Fig. 3 is attributed to unequal resonator and external optical path lengths. The achievement of $V = 1$, needed for a phased array, may require both resonator-length equalization and external-optical-path equalization.

It should be noted that the two outputs of the coupled laser system do not arise from oscillation between mirrors M_1 and M_3 ; the output from either laser ceases when its convex mirror (M_2 or M_4) is blocked. The lack of sensitivity of multiline fringe visibility to resonator length may imply that

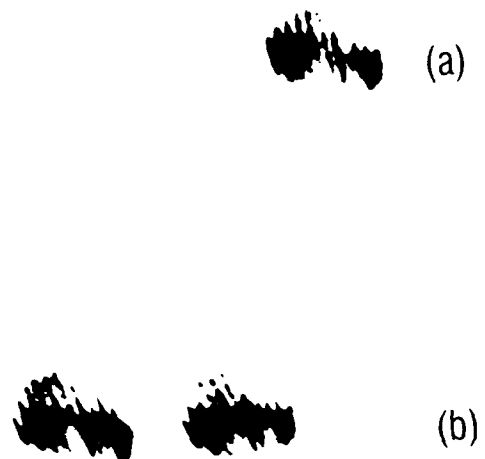


Fig. 2. Expanded thermal image of multiline near-field fringes: (a) lower resonator length $\sim 1.5 \text{ m} + 0.0 \mu\text{m}$, (b) lower resonator length $\sim 1.5 \text{ m} + 200 \mu\text{m}$.

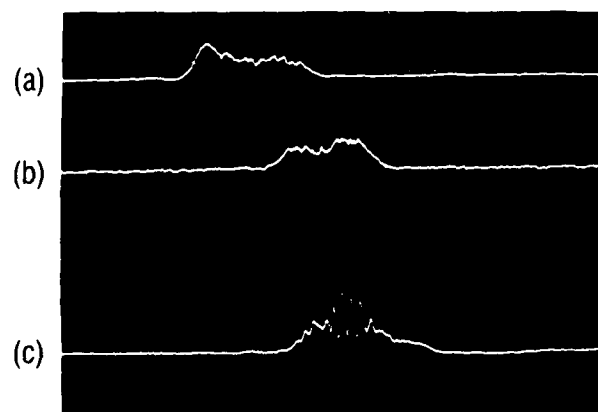


Fig. 3. Oscilloscope traces of multiline near-field scans: (a) lower beam only, (b) upper beam only, and (c) both beams overlapped.

the two lasers oscillate with a mode defined by the sum of the two resonator lengths plus the coupling path length. Longitudinal-mode beat-frequency measurements will be required in order to verify this.⁶

The present results may be explained by Mirels's⁴ theoretical model, about which he notes that stable coupled modes have less round-trip cavity loss than do unstable modes. When these modes compete for the same gain (as occurs in the present inhomogeneously broadened multilineline, multilongitudinal-mode HF laser medium), the stable modes will dominate and, in fact, quench the unstable modes. If the coupling is reduced from the present 20%, it is expected that the dominance of the stable, coupled modes will eventually diminish and the system will become more sensitive to resonator-length control. It should also be noted that the theory of Ref. 4 applies strictly to coupled Fabry-Perot resonators and not to unstable resonators such as those in the present experiments. Beam-splitter coupling between confocal unstable resonators implies the presence of converging waves, which effectively amplifies the intensity of the coupling radiation. Theories that incorporate these particular aspects of our experiments may explain our results. Further experiments⁶ have confirmed many of the above conclusions.

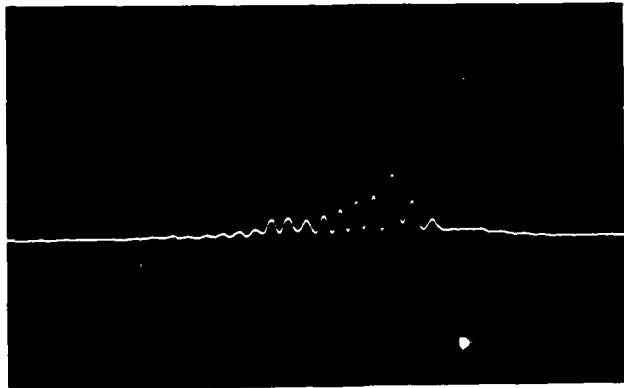


Fig. 4. Oscilloscope trace of $P_2(6)$ single-line fringe pattern.

REFERENCES

1. G. E. Palma and W. J. Fader, Proc. Soc. Photo-Opt. Instrum. Eng. 440, 153 (1983).
2. M. R. Spencer and W. E. Lamb, Jr., Phys. Rev. A 5, 893 (1972).
3. W. W. Chow, Opt. Lett. 10, 442 (1984).
4. H. Mirels, Appl. Opt. 25, 2130 (1986).
5. D. J. Spencer, H. Mirels, and D. A. Durran, J. Appl. Phys. 43, 1151 (1972).
6. J. M. Bernard, R. A. Chodzko, and H. Mirels, "Coupled multiline cw HF lasers: experimental performance," AIAA Paper No. 87-1448; to be published in AIAA J.

LABORATORY OPERATIONS

The Aerospace Corporation functions as an "architect-engineer" for national security projects, specializing in advanced military space systems. Providing research support, the corporation's Laboratory Operations conducts experimental and theoretical investigations that focus on the application of scientific and technical advances to such systems. Vital to the success of these investigations is the technical staff's wide-ranging expertise and its ability to stay current with new developments. This expertise is enhanced by a research program aimed at dealing with the many problems associated with rapidly evolving space systems. Contributing their capabilities to the research effort are these individual laboratories:

Aerophysics Laboratory: Launch vehicle and reentry fluid mechanics, heat transfer and flight dynamics; chemical and electric propulsion, propellant chemistry, chemical dynamics, environmental chemistry, trace detection; spacecraft structural mechanics, contamination, thermal and structural control; high temperature thermomechanics, gas kinetics and radiation; cw and pulsed chemical and excimer laser development including chemical kinetics, spectroscopy, optical resonators, beam control, atmospheric propagation, laser effects and countermeasures.

Chemistry and Physics Laboratory: Atmospheric chemical reactions, atmospheric optics, light scattering, state-specific chemical reactions and radiative signatures of missile plumes, sensor out-of-field-of-view rejection, applied laser spectroscopy, laser chemistry, laser optoelectronics, solar cell physics, battery electrochemistry, space vacuum and radiation effects on materials, lubrication and surface phenomena, thermionic emission, photo-sensitive materials and detectors, atomic frequency standards, and environmental chemistry.

Computer Science Laboratory: Program verification, program translation, performance-sensitive system design, distributed architectures for spaceborne computers, fault-tolerant computer systems, artificial intelligence, micro-electronics applications, communication protocols, and computer security.

Electronics Research Laboratory: Microelectronics, solid-state device physics, compound semiconductors, radiation hardening; electro-optics, quantum electronics, solid-state lasers, optical propagation and communications; microwave semiconductor devices, microwave/millimeter wave measurements, diagnostics and radiometry, microwave/millimeter wave thermionic devices; atomic time and frequency standards; antennas, rf systems, electromagnetic propagation phenomena, space communication systems.

Materials Sciences Laboratory: Development of new materials; metals, alloys, ceramics, polymers and their composites, and new forms of carbon; non-destructive evaluation, component failure analysis and reliability; fracture mechanics and stress corrosion; analysis and evaluation of materials at cryogenic and elevated temperatures as well as in space and enemy-induced environments.

Space Sciences Laboratory: Magnetospheric, auroral and cosmic ray physics, wave-particle interactions, magnetospheric plasma waves; atmospheric and ionospheric physics, density and composition of the upper atmosphere, remote sensing using atmospheric radiation; solar physics, infrared astronomy, infrared signature analysis; effects of solar activity, magnetic storms and nuclear explosions on the earth's atmosphere, ionosphere and magnetosphere; effects of electromagnetic and particulate radiations on space systems; space instrumentation.